

# Use of Short- and Long-Lived Rubidium Tracers for the Study of Transient Ischemia

Michael J. Shea, Richard A. Wilson, Christian M. deLandsheere, John E. Deanfield, Ian A. Watson, Malcolm J. Kensett, Terry Jones, and Andrew P. Selwyn

*MRC Cyclotron Unit and Cardiovascular Unit, Hammersmith Hospital, Royal Postgraduate Medical School, London, England*

Positron emission tomography (PET) with rubidium-82 ( $^{82}\text{Rb}$ ) has been developed to measure regional myocardial perfusion and to detect transient ischemia both in the experimental laboratory and in humans. There are known and separate contaminating effects of the  $^{82}\text{Rb}$  signal by disturbances in wall motion, wall thinning, and the partial volume effect that occur during transient ischemia. In nine anesthetized greyhounds, PET with  $^{82}\text{Rb}$  ( $T_{1/2} = 78$  sec) was used to determine the regional myocardial uptake of this cation during a control period that consisted of a mild stenosis of the left anterior descending coronary artery in the absence of ischemia (to limit reactive hyperemia), during 10 min of total occlusion and, finally, at 30 and 60 min of recovery with release of the occlusion but not of the stenosis. Separately, rubidium-81 ( $^{81}\text{Rb}$ ;  $T_{1/2} = 4.58$  hr) was given as a peripheral intravenous injection 2 hr before the study to allow this long-lived tracer to distribute in the potassium space of the myocardium. Observations during control and ischemia revealed marked decreases in  $^{82}\text{Rb}$  uptake ( $0.84 \pm 0.12$  to  $0.28 \pm 0.12$ ,  $p = 0.001$ ) in affected regions and were paralleled by similar decreases in microsphere blood flow ( $0.88 \pm 0.08$  to  $0.12 \pm 0.10$  ml/min/g,  $p = 0.003$ ), which gradually recovered by 60 min postischemia. Lesser decreases in  $^{81}\text{Rb}$  activity ( $0.84 \pm 0.11$  to  $0.76 \pm 0.17$ ,  $p = 0.83$ ) were observed in the same regions during ischemia, but these were immediately reversible. Separate in vitro postmortem experiments in eight rabbits confirmed a linear relationship between plasma and myocardial activities of stable potassium and  $^{81}\text{Rb}$  although there was a greater concentration of  $^{81}\text{Rb}$  in the myocardium than in the plasma relative to potassium ( $y = -3.29 \pm 0.79 x$ , s.e.e. 1.91,  $r = 0.95$ ). These studies demonstrate that if  $^{81}\text{Rb}$  is given intravenously to distribute into the potassium pool, tomograms of the heart may be recorded to measure the potassium-rich mass of myocardium providing information about the acute effects of wall thinning during ischemia. Rubidium-81 used in this way may be helpful in assessing the effects of wall thinning and/or scar when other tracers are being used to assess perfusion or metabolism.

J Nucl Med 28:989-997, 1987

The size of myocardial infarction and assessment of regional myocardial perfusion and metabolism are two important measurements for diagnosis and research, which can be obtained by positron emission tomography (PET) (1-3). However, measuring tracer concentrations in the myocardium is limited by both the partial volume effect (4) and the unknown admixture of viable and scarred myocardium. Measurements of perfusion and metabolism could be improved if the geometric distribution of myocardium under study could be in-

dependently described. The purpose of this report is to describe the use of short- and long-lived rubidium tracers to study the combined disturbances of perfusion and ventricular geometry that occur during acute ischemia. Rubidium-82 ( $^{82}\text{Rb}$ ;  $T_{1/2} = 78$  sec) is used to measure regional myocardial perfusion (5). Rubidium-81 ( $^{81}\text{Rb}$ ;  $T_{1/2} = 4.58$  hr) is used in parallel to assess the effect of changing ventricular geometry during transient regional ischemia.

## MATERIALS AND METHODS

### Experiments in Dogs

*Surgical preparation.* Nine greyhounds (21-33 kg) were treated with amiodarone hydrochloride 10 mg/kg/day orally

Received Dec. 9, 1985; revision accepted Dec. 23, 1986.

For reprints contact: Michael J. Shea, MD, University of Michigan Hospital, Cardiology Div. TC 3910, Ann Arbor, MI 48109-0366.

for 3–5 days before surgery to prevent lethal ventricular arrhythmias during myocardial ischemia (vide infra). The animals were anesthetized with 0.3 mg/kg i.v. thiopentone sodium, intubated, and ventilated. Anesthesia was maintained with i.v. alpha-chloralose (30 mg/kg loading dose followed by 10 mg/kg/hr). Polyethylene cannulae were placed in a femoral artery and vein. A left thoracotomy was performed and the heart was suspended in a pericardial cradle. A polyethylene cannula was placed in the left atrium via the left atrial appendage. The mid-left anterior descending coronary artery (LAD) was dissected free and a micrometer-adjustable mechanical occluder was placed around the artery. An electromagnetic flowprobe was positioned proximal to the occluder.

Mean arterial and left atrial pressure, phasic LAD flow, and a lead II electrocardiogram were monitored, and the mean LAD flow signal was also displayed digitally.

**PET with  $^{82}\text{Rb}$  and  $^{81}\text{Rb}$ .** Rubidium-81 was produced using a technique previously described (6). Two hours before tomography (during surgery) 2–4 mCi of  $^{81}\text{Rb}$  as chloride was given intravenously. The PET camera had a spatial resolution 15 mm full-width half-maximum (FWHM). A laser was used to align the image plane with a mid-left ventricular transaxial slice used for all subsequent tomograms.

A 300-sec transmission scan using an external ring source of germanium-68 ( $^{68}\text{Ge}$ ) was recorded, followed by a second transmission scan with no ring source. This latter scan was decay-corrected and subtracted from the first transmission scan to correct for the  $^{81}\text{Rb}$  in the dog when estimating attenuation correction. Two to 4 million counts were typically collected in transmission tomograms.

Fifteen millicuries of  $^{82}\text{Rb}$  ( $T_{1/2} = 78$  sec) in 0.9% NaCl was continuously eluted from a strontium-82 ( $^{82}\text{Sr}$ )/ $^{82}\text{Rb}$  generator (7–10) at 10 ml/min. A peripheral intravenous infusion produces an equilibrium of activity in the arterial circulation—at this point a 60-sec equilibrium was recorded. Equilibrium tomograms recorded 300,000–500,000 counts. A second myocardial tomogram was recorded 30–150 sec after stopping the infusion to record the regional myocardial activity of the tracer. This latter tomogram contained 300,000–500,000 counts. After reconstruction the regional myocardial uptake of  $^{82}\text{Rb}$  was calculated using the arterial concentrations from the equilibrium scan and the regional myocardial concentration from the myocardial scan (5). The regional myocardial uptake of  $^{82}\text{Rb}$  represents the regional myocardial concentration achieved, which has been standardized by the measured arterial input for that tomogram. This is a product of flow (ml/min/g) and extraction of  $^{82}\text{Rb}$  and is expressed as a fraction (i.e., myocardial to arterial activity of  $^{82}\text{Rb}$ ).

**Microspheres.** Carbonized gamma microspheres (9  $\mu\text{m}$ ) labeled with cobalt-57 ( $^{57}\text{Co}$ ), cerium-141 ( $^{141}\text{Ce}$ ), tin-113 ( $^{113}\text{Sn}$ ), ruthenium-103 ( $^{103}\text{Ru}$ ), or scandium-46 ( $^{46}\text{Sc}$ ) were injected into the left atrium for measurement of regional myocardial blood flow. A timed arterial withdrawal from the femoral artery served as the reference sample (11).

**Experimental protocol.** After the transmission scans, the following measurements were made:

1. An emission tomogram of  $^{81}\text{Rb}$  (200 sec).
2. Emission tomograms during and after i.v. infusion of  $^{82}\text{Rb}$ .
3. Left atrial injection of reference microspheres with a timed arterial withdrawal.

4. Heart rate, blood pressure, LAD flow, and electrocardiogram.

The above set of measurements were made:

1. During a control period when the LAD was stenosed to decrease the reactive hyperemic response to a 10-sec complete occlusion by more than 80% while leaving resting flow unchanged (no change in left atrial pressure or electrocardiogram).

2. During 10 min of complete occlusion of the LAD, (the LAD was then reperfused but the mechanical occluder was allowed flow to return only to the control levels without allowing hyperemia).

3. Thirty minutes after release of the occlusion to the flow of preocclusion stenosis.

4. Sixty minutes after the release of occlusion.

At the end of each experiment animals were killed with 10% KCl after transfixing hearts with externally inserted metal skewers in the plane of the tomographic slice. A 15-mm myocardial slice within the tomographic plane was then dissected free. Both the caudad and cephalad sides were traced on clear acetate overlays outlining borders, dimensions, and orientation.

After outlining the heart borders on acetate, the remaining caudad and cephalad portions of the heart were sliced into 15-mm sections. These sections were then pan-stained with triphenyltetrazolium chloride to assess the presence or absence of infarction (12).

**Analysis of tomograms.** Rubidium-81 contamination was subtracted from each  $^{82}\text{Rb}$  tomogram and the regional myocardial uptake of  $^{82}\text{Rb}$  was then calculated (11).

Following reconstruction, the myocardium was identified by enclosing all pixels with values 50% of the peak value. In the first tomogram of each animal, large anatomic regions of interest (1.37  $\text{cm}^2$ ) were identified from posterior wall, free wall, anterior wall, and interventricular septum (two regions) and the same regions of interest were then used for measurements during the serial changes from control through ischemia and recovery.

A mean of ten measurements of regional left ventricular wall thickness was made for each segment from acetate tracings and were used to correct the measurements of regional myocardial uptake of  $^{82}\text{Rb}$  for the underestimations of count rate recovery (4). The corrected values were used for comparison with microsphere flow (in vitro measurements of tissue samples). Separate phantom studies were performed to obtain recovery coefficients.

**Regional myocardial blood flow.** After removing the inplane myocardial slice, the tissue samples and reference arterial samples were then counted and the regional myocardial activity per unit weight was used with the arterial reference technique to calculate regional myocardial blood flow in ml/min/g (11). The regional myocardial segments were matched with the  $^{82}\text{Rb}$  and  $^{81}\text{Rb}$  tomograms and flow calculated from a mean of four to eight measurements in each segment.

#### Experiments in Rabbits

Eight New Zealand white rabbits (2–2.5 kg) were given 0.3–0.8 mCi  $^{81}\text{Rb}$  as chloride by way of an ear vein. Two hours later the animals were anesthetized with intravenous Hypnorm (fentanyl-promethazine) and their hearts and 20 ml of blood were removed. The blood samples were centrifuged and

plasma  $^{81}\text{Rb}$  activity was determined in a calibrated NaI well counter (counts/sec/ml) and the plasma potassium concentrations were measured.

Three 1-g myocardial tissue samples were blotted and dissolved in 5 ml of concentrated nitric acid at 40°C for 90 min (13). The tissue was manually agitated and diluted with 5 ml of 0.9% NaCl. A 2-ml aliquot was used to measure both  $^{81}\text{Rb}$  activity and potassium concentration. Back dilution with sample weights allowed the calculation of myocardial potassium in meq/l.

**Statistical methods.** The regional myocardial uptake of  $^{82}\text{Rb}$ , the regional myocardial activity of  $^{81}\text{Rb}$ , and microsphere flow are expressed as mean  $\pm$  1 s.d. Changes in the regional myocardial uptake of  $^{82}\text{Rb}$ , activity of  $^{81}\text{Rb}$ , and microsphere flow for each myocardial segment were assessed initially with paired t-tests (14). Inter- and intragroup comparisons between  $^{82}\text{Rb}$ ,  $^{81}\text{Rb}$ , and microsphere flow in the affected anteroapical segment were analyzed using analysis of variance and covariance with repeated measures (15). The relationship between the regional myocardial uptake of  $^{82}\text{Rb}$  and microsphere flow was assessed by three-parameter logistic curve analysis (16). The relationship between potassium and Ru in the plasma and Ru in the myocardium for the rabbit experiments was analyzed using linear regression (14).

## RESULTS

### Experiments in Dogs

In the nine separate dog experiments, heart rate, blood pressure, and the electrocardiogram did not change by more than  $\pm$  5% during the experiments except for a transient increase in heart rate and decrease in blood pressure accompanied by ischemic ST-T changes during the 10 min of LAD occlusion.

Under control conditions, nine comparisons were made between  $^{82}\text{Rb}$  uptake,  $^{81}\text{Rb}$  activity and microsphere flow. Similarly, during LAD occlusion, nine comparisons were made between  $^{82}\text{Rb}$  uptake,  $^{81}\text{Rb}$  activity and microsphere flow. At 30 min after reperfusion of the previously occluded LAD, only five comparisons between all three parameters were recorded because four experiments were ended by ventricular arrhythmias. One other experiment was lost between 30 and 60 min, providing four comparisons at 60 min.

The first six of nine dogs underwent staining with triphenyltetrazolium chloride to detect the presence or absence of infarction. For all six animals, staining was uniform indicating presence of viable tissue at a macroscopic level. No evidence for infarction was present.

**Tomography using  $^{81}\text{Rb}$ —volume marker of viable myocardium.** Clear delineation of myocardium was seen in all experiments with a ratio of peak myocardial counts/pixel to left ventricular cavity at  $6.9 \pm 2.7:1$  and peak myocardial counts to lung ratio of  $31 \pm 8:1$ .

The distribution of  $^{81}\text{Rb}$  activity within the myocardial tomograms is shown in Figure 1 and the effects of transient occlusion of the LAD are shown in Figures 1–5 and Table 1. With ischemia, the affected anteroapical

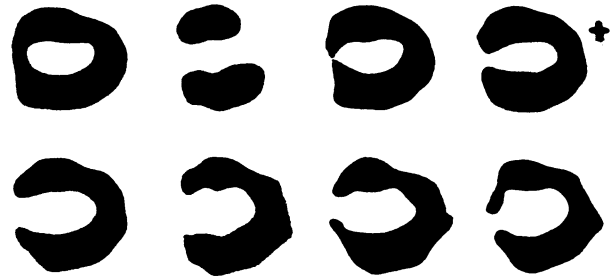


**FIGURE 1**

An individual experiment with tomograms of  $^{82}\text{Rb}$  uptake and  $^{81}\text{Rb}$  activity. The top four tomograms from left to right show the regional myocardial uptake of  $^{82}\text{Rb}$  that is (a) uniform in control, (b) shows severe reduction in the anteroapical segment during left anterior descending coronary artery occlusion, (c) nearly recovered at 30 min and (d) completely recovered by 60 min. The bottom four tomograms of  $^{81}\text{Rb}$ , representing viable myocardium, show, from left to right, minimal change in activity in the same segment. Wall thinning and/or change in geometry did not contribute to the signals of cation uptake and flow in this case. The orientation of each tomogram is: 9 o'clock, mitral orifice; 12 o'clock, left ventricular free wall; 3 o'clock, anterior myocardium; 6 o'clock, interventricular septum.

segment demonstrates a 15% reduction in  $^{81}\text{Rb}$  activity ( $p = 0.12$ ). At 30 min the  $^{81}\text{Rb}$  activity is not significantly different than control values. If the affected segment is expressed as a percentage of a remote, normal segment, similar changes are observed with a 10% reduction in  $^{81}\text{Rb}$  activity during ischemia ( $p = 0.83$ ) (Table 1).

**Tomography using  $^{82}\text{Rb}$ —perfusion marker.** Figure 1 shows the homogeneous regional myocardial uptake of

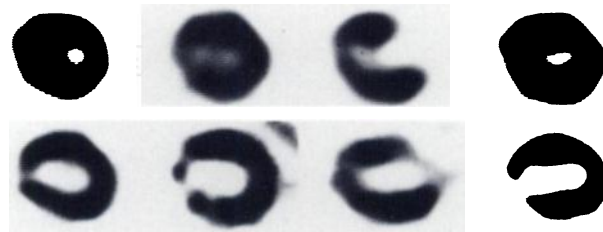


**FIGURE 2**

An individual experiment with tomograms of  $^{82}\text{Rb}$  uptake and  $^{81}\text{Rb}$  activity. The top four tomograms, from left to right, show the regional myocardial uptake of  $^{82}\text{Rb}$  that is (a) uniform in an initial control period (before the mild stenosis was applied), (b) uniform during the mild stenosis, (c) severely reduced in the anterior heart during left anterior descending coronary artery occlusion, and (d) recovered at 60 min after release of the occlusion. The bottom four tomograms of  $^{81}\text{Rb}$  do show a change in activity in the same segment during ischemia (the third tomogram) but this is reversible by 60 min after release of the occlusion (fourth tomogram). The  $^{81}\text{Rb}$  was given 2 hr before the study and separately represents the potassium pool demonstrating wall thinning during ischemia. The orientation for these tomograms is the same as for Figure 1.

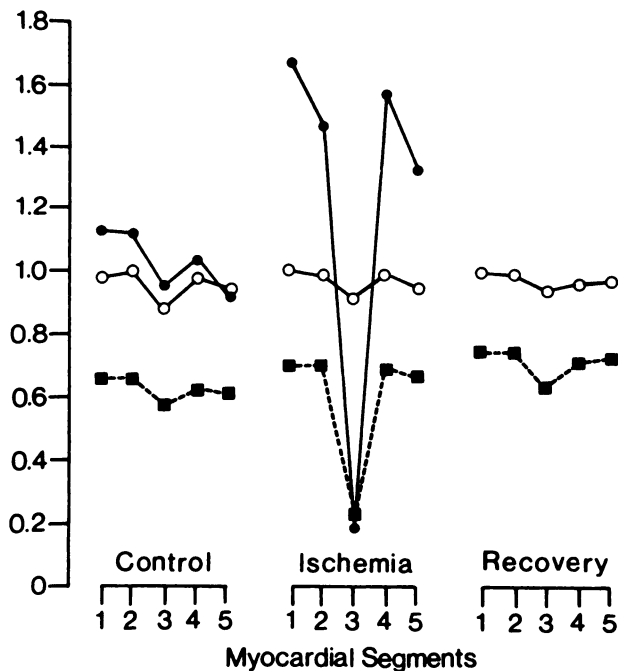


**FIGURE 3**

An example of the quantitation of the tomographic signals and microsphere flow from five myocardial segments in a representative experiment. During ischemia there are marked decreases in  $^{82}\text{Rb}$  uptake and microsphere flow while the volume signal from  $^{81}\text{Rb}$  shows no separate effect. (●—●) Microsphere flow [ml/min/g]; (○—○)  $^{81}\text{Rb}$  activity  $\times 10^3$ ; (■—■)  $^{82}\text{Rb}$  uptake [ml/min/g  $\times$  E].

$^{82}\text{Rb}$ , the homogeneous regional myocardial activity of  $^{81}\text{Rb}$ , and uniform microsphere flow during a control period. After LAD occlusion there is a marked fall in uptake of  $^{82}\text{Rb}$  and microsphere flow in the anteroapical segment of the heart. The  $^{81}\text{Rb}$  signal shows no appreciable change in the same segment. In Figure 2, from

another experiment, after LAD occlusion there is again a marked decrease in  $^{82}\text{Rb}$  uptake and microsphere flow to the anterior heart, whereas, the  $^{81}\text{Rb}$  tomograms show a smaller change in the same segment, which is reversible after release of the occluder. The absolute values of regional myocardial uptake of  $^{82}\text{Rb}$  are shown in Figure 5. There are marked decreases in  $^{82}\text{Rb}$  uptake ( $>70\%$ ) that are paralleled by decreases in microsphere flow ( $>80\%$ ) during ischemia. These changes are significantly different from control: For  $^{82}\text{Rb}$  uptake  $p = 0.001$  (Greenhouse–Geisser probability 0.002) and for microsphere flow  $p = 0.003$  (Greenhouse–Geisser probability 0.034). Table 1 demonstrates similar results with the  $^{82}\text{Rb}$  uptake and microsphere flow of the affected anteroapical segment expressed as a percentage of the peak value in a remote segment.

*Relationship between cation uptake and microsphere flow.* The relationship between  $^{82}\text{Rb}$  uptake and microsphere flow is plotted in Figure 6. For this data the  $^{82}\text{Rb}$  uptake values have been partial volume corrected. This data was best expressed using nonlinear regression with a three-parameter logistic model where

$$y = \frac{0.89 e^{-2.56x}}{1 + e^{-2.56x}} \quad (1)$$

( $r = 0.74$ , s.e.e. 0.14).

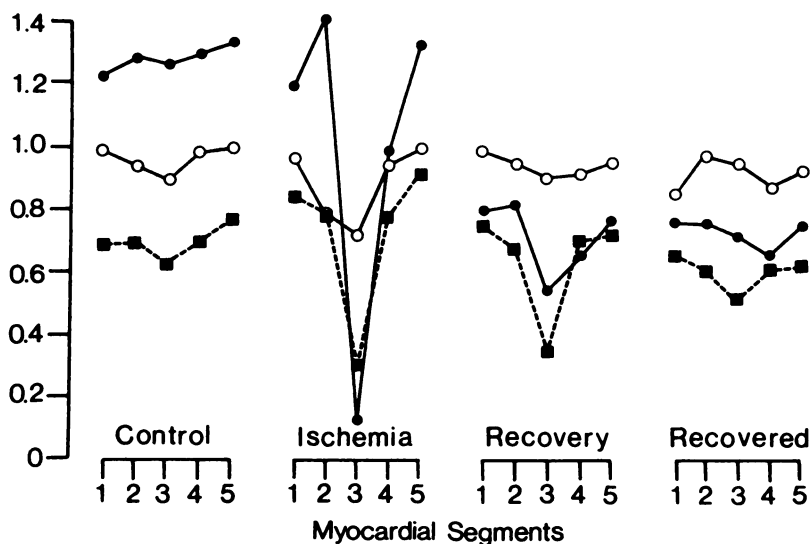
At low flow rates or during ischemia the relationship between cation uptake and flow is nearly linear, suggesting that  $^{82}\text{Rb}$  uptake is a reliable perfusion signal in these conditions. At high flow rates cation uptake underestimates flow, as has been demonstrated by other investigators (17,18).

#### Experiments in Rabbits

The plasma potassium values were  $4.2 \pm 0.7$  mEq/l. The myocardial values were  $89.0 \pm 9.1$  mEq/g. Simi-

**FIGURE 4**

An example of the quantitation of the tomographic signals and microsphere flow from five myocardial segments in a representative experiment. During ischemia there are marked reversible decreases in  $^{82}\text{Rb}$  uptake and microsphere flow accompanied by a much smaller, reversible change in  $^{81}\text{Rb}$  activity which represents the potassium-rich and viable myocardium. (●—●) Microsphere flow [ml/min/g]; (○—○)  $^{81}\text{Rb}$  activity  $\times 10^3$ ; (■—■)  $^{82}\text{Rb}$  uptake [ml/min/g  $\times$  E].



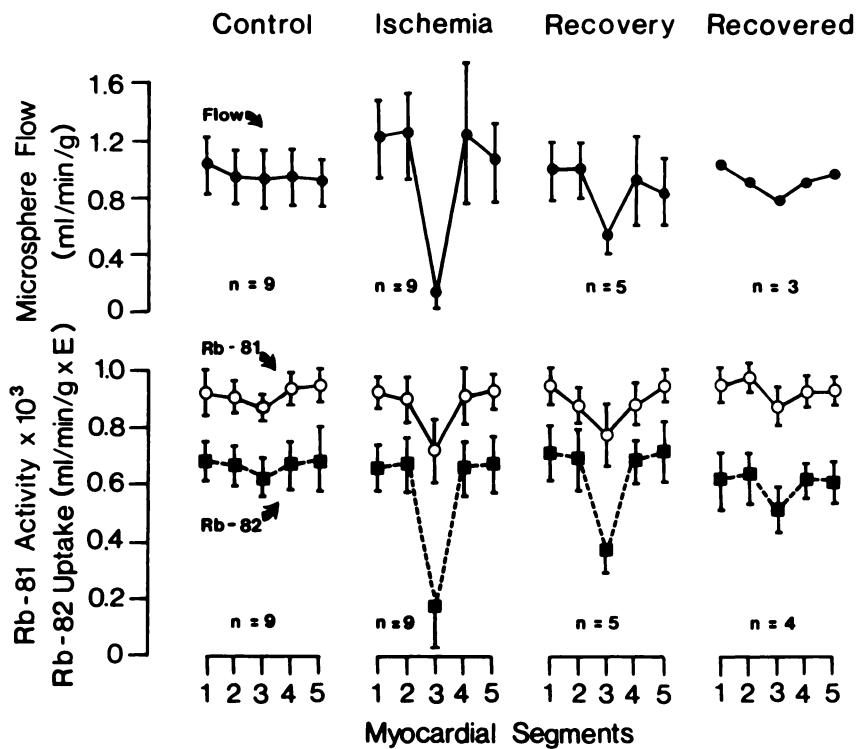


**FIGURE 5** These graphs plot regional myocardial blood flow, cation uptake ( $^{82}\text{Rb}$ ) and fractional distribution of  $^{81}\text{Rb}$  activity (counts/pixel/200 sec scan) in control, during ischemia (occlusion of the left anterior descending coronary artery), 30 min after release of the occlusion ("recovery") and 60 min after release of the occlusion ("recovered") for all the completed experiments. Microsphere flow and  $^{82}\text{Rb}$  uptake are markedly decreased during ischemia and recovery as compared to control. There is considerably less change in the  $^{81}\text{Rb}$  signal during ischemia. However, the changes in viable tissue ( $^{81}\text{Rb}$  signal) due to wall thinning must be considered when measuring ischemic perfusion with tracers such as  $^{82}\text{Rb}$  (mean  $\pm$  s.d.).

larly, data for plasma  $^{81}\text{Rb}$  and myocardial  $^{81}\text{Rb}$  were:  $42.8 \pm 21.7$  counts/sec/ml for plasma and  $1,565 \pm 817$  counts/sec/ml. The greater variation in the  $^{81}\text{Rb}$  counts reflect different administered doses of  $^{81}\text{Rb}$ . A ratio was made of  $^{81}\text{Rb}$  (counts/sec/ml) and potassium (mEq/g) in plasma and a similar ratio was made for the myocardium. Figure 7 demonstrates this relationship assessed by linear regression analysis. The data is expressed by the equation:

$$y = -3.29 \pm 0.79 \times (\text{s.e.e. } 196, \\ r = 0.95 \text{ (} p < 0.001 \text{)}). \quad (2)$$

There is a clear relationship between potassium and  $^{81}\text{Rb}$  in the plasma and potassium and  $^{81}\text{Rb}$  in the

myocardium with a greater concentration of  $^{81}\text{Rb}$  in the myocardium than in the plasma.

## DISCUSSION

In PET, the separate contributions from wall thinning and changes in geometry during an ischemic event cannot be assessed and, thus, interfere with quantitation (19-22). Information gained separately from a tracer in the same geometry of detection as used to assess perfusion could provide data to at least partially alleviate problems in quantitation due to wall thinning (2, 23).

These experiments have shown that  $^{81}\text{Rb}$  will con-

**TABLE 1**  
Ratio of Affected Anteroapical Myocardial Region to Peak Value in a Normal Remote Myocardial Region During Differing Time Periods

	Control (n = 9)	Ischemia (n = 9)	Recovery (30 min postischemia) (n = 5)	Recovered (60 min postischemia) (n = 4)
$^{82}\text{Rb}$ uptake	$0.84 \pm 0.12$	$0.28 \pm 0.12^*$	$0.53 \pm 0.08^\ddagger$	$0.80 \pm 0.06$
Microsphere flow	$0.88 \pm 0.08$	$0.12 \pm 0.10^\dagger$	$0.52 \pm 0.16^\ddagger$	$0.87 \pm 0.12$
$^{81}\text{Rb}$ activity	$0.84 \pm 0.11$	$0.76 \pm 0.17^\ddagger$	$0.76 \pm 0.20^\ddagger$	$0.86 \pm 0.11$

All values are mean  $\pm$  s.d.

\*, †, ‡, and § were analyzed with repeated measures analysis of variance.

\*  $p = 0.001$  (Greenhouse-Geisser probability 0.005) versus control.

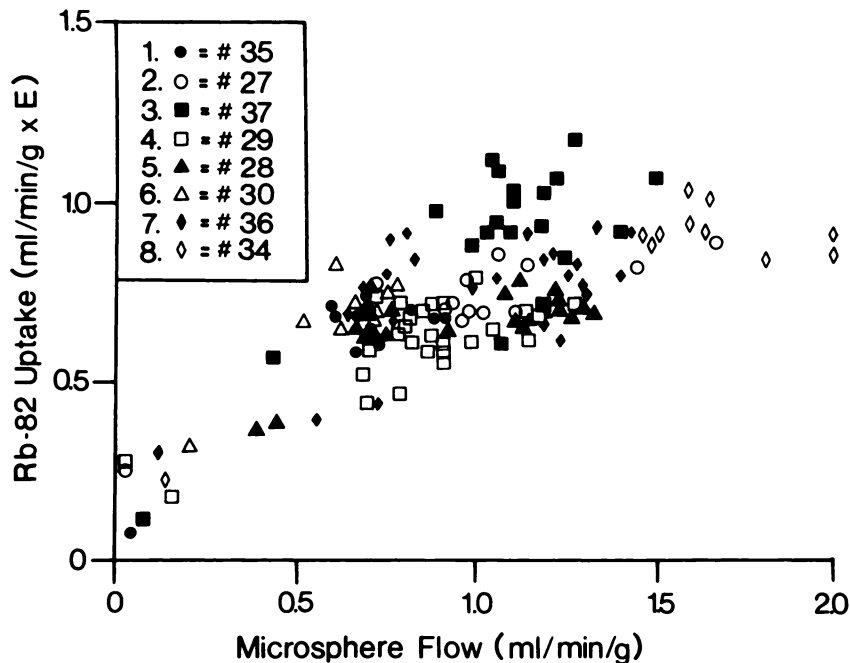
†  $p = 0.003$  (Greenhouse-Geisser probability 0.015) versus control.

‡  $p = 0.83$  versus control.

§  $p = \text{N.S.}$  versus control conditions.

**FIGURE 6**

The relationship between regional myocardial  $^{82}\text{Rb}$  uptake ( $\text{ml}/\text{min}/\text{g} \times \text{E}$ ) and regional myocardial blood flow ( $\text{ml}/\text{min}/\text{g}$ ). Rubidium-82 uptakes were calculated after subtracting the  $^{81}\text{Rb}$  data and correcting for the partial volume effect (which results in decreases in count recovery as a function of wall thickness). The nonlinear relationship means that ischemia and low flow states are well represented by cation uptake but higher flow rates may be underestimated. ( $n = 130, r = 0.74$ ).



concentrate in the myocardial potassium pool and provide tomograms for several hours (24). The steady decline in myocardial activity of  $^{81}\text{Rb}$  probably represents the continuing equilibration of the tracer into the potassium pools (13,25,26). Nevertheless, at 2 hr postinjection equilibration in plasma and myocardium is largely complete (13,27).

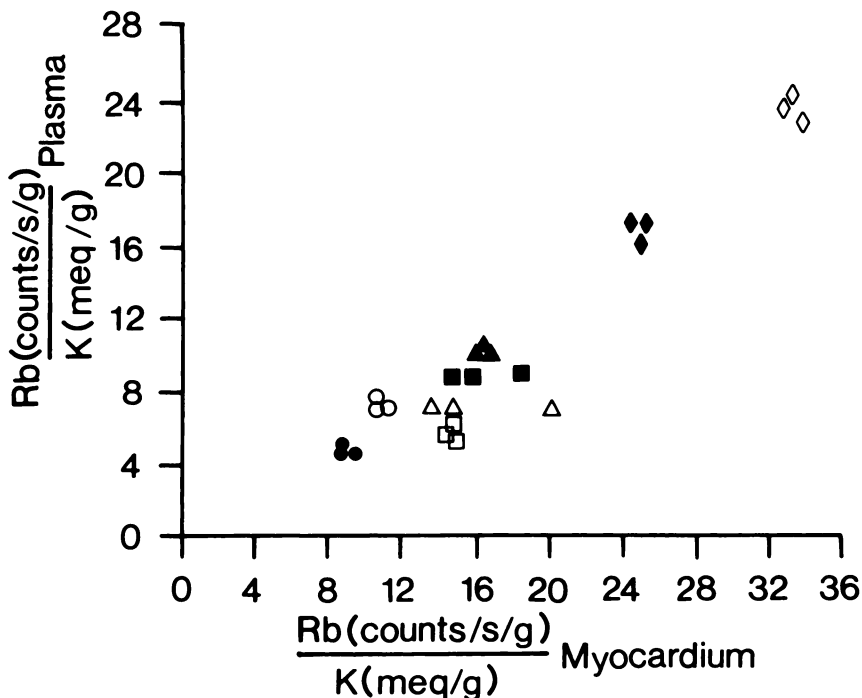
Left anterior descending artery occlusion produced profound regional decreases in uptake of  $^{82}\text{Rb}$  and flow in the affected segment, with partial recovery at 30 min

and almost complete recovery 60 min after a 10-min period of ischemia. The  $^{81}\text{Rb}$  tomograms also showed immediate but much smaller changes during LAD occlusion; these, however, reverted to normal within minutes of reperfusion and long before the recovery of the perfusion scans using  $^{82}\text{Rb}$ .

Previous studies of the kinetics of  $^{81}\text{Rb}$  indicate that its equilibrium distribution is closely related to the potassium pool in each tissue (28-31). A high intracellular concentration of potassium is characteristic of

**FIGURE 7**

Two hours after i.v. injection of  $^{81}\text{Rb}$  in rabbits, the ratio of potassium and  $^{81}\text{Rb}$  in the plasma shows a linear relationship with the same ratio in the myocardium ( $n = 24, r = 0.95$ ). The offset probably means that  $^{81}\text{Rb}$  occupies more of the potassium pool in the myocardium than in the plasma. It may be possible to estimate the myocardial potassium with blood samples and external detection of myocardial  $^{81}\text{Rb}$  if this linear relationship exists in man. (○) = #59; (●) = #60; (□) = #61; (■) = #62; (△) = #63; (▲) = #64; (◇) = #65; (◆) = #66.



healthy myocardium, which can be lost in heart failure and infarction. The transient changes in  $^{81}\text{Rb}$  activity seen in some of these experiments occurred within 2 min of LAD occlusion and this is unlikely to be due to a major loss of  $^{81}\text{Rb}$  from cells. Rubidium-81 may have been lost during ischemia but returned during reperfusion; overall viability was maintained. In addition, a number of experiments showed no change and all the experiments showed recovery within 30 min after LAD occlusion release. This rapid and reversible change in  $^{81}\text{Rb}$  activity is much more likely to be due to wall thinning and changes in geometry that are known to occur during acute transient regional myocardial ischemia than a significant change in intracellular potassium or  $^{81}\text{Rb}$ . In experimental models, however, complete occlusion of a coronary artery with severe ischemia will only show a significant decrease in tissue potassium 3 or 4 hr later, probably due to the reduction in flow when the activity of Na/K ATPases is no longer sustained. In contrast, if coronary occlusion is followed by reperfusion then significant transient alterations in cellular potassium can occur. Most previous work in this regard has shown that the ability to concentrate and/or recover the intracellular potassium is closely related to viability of myocardium (23,32-36).

Previous research suggests that when cations like  $^{81}\text{Rb}$  are distributed hours after administration, they represent the potassium pool (23,30,32). The rabbit experiments confirmed that there is a close relationship between potassium and  $^{81}\text{Rb}$  in the plasma and potassium and  $^{81}\text{Rb}$  in the myocardium with greater concentration of  $^{81}\text{Rb}$  in the potassium pool of the muscle than in the plasma (27). Clearly, if potassium and  $^{81}\text{Rb}$  can be measured in the plasma and the  $^{81}\text{Rb}$  activity can be measured in the myocardium (by tomographic scanning), then the myocardial concentration of potassium might be estimated considering the linear relationship shown in the rabbit. This relationship would have to be tested in humans.

### Clinical Implications

The smaller, immediate changes in  $^{81}\text{Rb}$  activity during ischemia suggest that wall thinning can be separately assessed and accounts for a small, variable but potentially important proportion of the regional abnormalities recorded by an external detector using perfusion tracers such as  $^{82}\text{Rb}$ .

Previous clinical studies have not addressed this problem. Echocardiography is one potential solution. This technique has been applied successfully in the open-chest dog to provide wall thickness corrections for PET measurements of regional blood flow (37). Other imaging techniques could be used for single measurements of ventricular geometry but would have to be isolated in time. Serial studies of physiologic events of interest

with rapidly changing ventricular geometry would be ill-suited to moving the patient into and out of separate imaging devices. The attraction of  $^{81}\text{Rb}$  is that this radionuclide could be present as a "background tracer." Rubidium-81 could be given 2 hr before a study in patients and used in parallel with tracers that look at perfusion or metabolism. The radiation dose is not excessive for clinical work, for example, 2 mCi i.v.  $^{81}\text{Rb}$  plus four estimates of  $^{82}\text{Rb}$  uptake would give less than 80 mrem to the whole body and less than 170 mrem to the kidneys in a 70-kg man. In these experiments the  $^{82}\text{Rb}$  activity was always more than seven times the  $^{81}\text{Rb}$  activity and the short half-life of  $^{82}\text{Rb}$  ( $t_{1/2} = 78$  sec) allows the  $^{81}\text{Rb}$  activity to be assessed separately. In the present experiments the advantage of the dual isotope approach is that dynamic changes in perfusion may be assessed with  $^{82}\text{Rb}$ , whereas, the static volume data can be recorded by  $^{81}\text{Rb}$ . Because the detection geometry is similar for both tomographic slices, the problems of partial volume are partly overcome when expressing data in this way.

This study emphasizes the need for an assessment of wall thickness (or thinning) when tracers are used to study acute ischemia in patients. The dual use of  $^{81}\text{Rb}$  and  $^{82}\text{Rb}$  may be one solution in certain circumstances. This approach would be limited in any patient with previous infarction, in patients with prolonged recovery from previous ischemic insults, or in the theoretical case of a patient with a slow rate of cation equilibration or other defect in transmembrane cation transport.

### CONCLUSION

During 10 min of transient myocardial ischemia there is a marked reduction (>70%) in regional myocardial perfusion as assessed by PET measurements of  $^{82}\text{Rb}$  uptake and mirrored by similar reductions in microsphere blood flow. The disturbance in  $^{82}\text{Rb}$  uptake is prolonged but recovers by 60 min. At the same time, measurements of  $^{81}\text{Rb}$  activity, a marker of the potassium-rich myocardium, demonstrate a much smaller (20%) momentary decrease in activity with early and complete recovery within minutes after ischemic provocation. The dual isotope approach provides information on regional perfusion and cation uptake ( $^{82}\text{Rb}$  signal), whereas, the  $^{81}\text{Rb}$  signal contributes important information regarding the separate problems of disturbed wall motion and wall thinning, both of which combine to contaminate the perfusion signal. Thus, ischemia with its attendant geometric changes in the myocardium produces a small, variable effect on measurements of regional myocardial perfusion. Clinical studies in patients will have to consider this effect.

### NOTE

\* ECAT II, Ortec, Inc., Oak Ridge, TN.

## ACKNOWLEDGMENTS

This work was supported by grants from the Medical Research Council of Great Britain and the British Heart Foundation. The parent strontium-82 of the  $^{82}\text{Sr}/^{82}\text{Rb}$  generator was a kind gift from the Clinton P. Anderson Meson Physics facility at the Los Alamos Scientific Laboratory, NM. Part of the statistical analysis was supported by GCRC Grant #3MO1RR042 (CLINFO) to the University of Michigan. M.J. Shea is a Clinician-Scientist Awardee of the American Heart Association, supported in part by the Michigan Heart Association. R.A. Wilson is a British-American Heart Research Fellow of the American Heart Association and Fulbright Scholar. C.M. deLandsheere is a NATO Fellow. J.E. Deanfield is a Medical Research Council (UK) Training Fellow.

The authors thank Judy Seeger, Terri Glazier, and Joan Stea for excellent secretarial help. We gratefully acknowledge the technical assistance of A. Jonathan, G. Forse, M. Almeida, A. Lewis, N. Anderson, R. Bartlett, and S. Hedges, and the statistical help of S. Schmaltz, Ph.D.

## REFERENCES

1. Pohost GM, Zir LM, Moore RH, et al. Differentiation of transient ischemia from infarcted myocardium by serial imaging after a single dose of thallium-201. *Circulation* 1972; 55:294-302.
2. Falsetti HL, Marcus ML, Kerber RE, et al. Quantification of myocardial ischemia and infarction by left ventricle imaging. *Circulation* 1981; 63:747-755.
3. Schelbert HR, Phelps ME. Positron computed tomography for the *in vivo* assessment of regional myocardial function. *J Molec Cell Cardiol* 1984; 16:683-693.
4. Hoffman EJ, Huang SC, Phelps ME. Quantitation in positron emission computed tomography. *J Comput Assist Tomogr* 1979; 3:299-307.
5. Selwyn AP, Allan RM, L'Abbate A, et al. Relation between regional myocardial uptake of rubidium-82 and perfusion: absolute reduction of cation uptake in ischemia. *Am J Cardiol* 1982; 50:112-121.
6. Clark JC, Horlock PL, Watson IA. Krypton-81m generators. *Radiochem Radioanal Lett* 1976; 25:245-254.
7. Horlock P, Clark J, O'Brien HA, et al. The preparation of a rubidium-82 radionuclide generator. *J Radioanal Chem* 1981; 64:257-265.
8. Yano Y, Budinger TF, Chiang G. Evaluation and application of alumina-based Rb-82 generators charged with high levels of Sr-82/85. *J Nucl Med* 1979; 20:961-966.
9. Neirinckx RD, Kronauge JF, Gennaro GP, et al. Evaluation of inorganic absorbents for the rubidium-82 generators: I. Hydrated  $\text{SnO}_2$ . *J Nucl Med* 1982; 23:245-249.
10. Waters SL, Butler KR, Clark JC, et al. Radioassay problems associated with the clinical use of a  $^{82}\text{Rb}$  radionuclide generator. *Intl J Nucl Med Biol* 1983; 10:69-74.
11. Heymann MA, Payne BD, Hoffman JIE, et al. Blood flow measurements with radionuclide-labelled particles. *Progr Cardiovasc Dis* 1977; 20:55-79.
12. Shea MJ, Murtagh JJ, Jolly SR, et al. Beneficial effects of nafazatrom on ischemic reperfused myocardium. *Eur J Pharmacol* 1984; 102:63-70.
13. Love WD, Romney RB, Burch GE. A comparison of the distribution of potassium and exchangeable rubidium in the organs of the dog, using rubidium<sup>86</sup>. *Circ Res* 1954; 2:112-122.
14. Armitage P. Statistical methods of medical research. London: Blackwell Scientific Publications, 1971:116-126, 150-155.
15. Winer BJ. Statistical principles in experimental design. New York: McGraw-Hill, 1971:261-305.
16. Volund A. Application of the four parameter logistic model to bioassay: comparison with slope ratio and parallel line models. *Biometrics* 1978; 34:357-365.
17. Prokop EK, Strauss HW, Shaw J, et al. Comparison of regional myocardial perfusion determined by ionic potassium-43 to that determined by microspheres. *Circulation* 1974; 50:978-984.
18. Mays E Jr, Cobb FR. Relationship between regional myocardial blood flow and thallium-201 distribution in the presence of coronary artery stenosis and dipyridamole-induced vasodilation. *J Clin Invest* 1984; 73:1359-1366.
19. Theroux P, Franklin D, Ross J Jr, et al. Regional myocardial function during acute coronary occlusion and its modification by pharmacological agents in the dog. *Circ Res* 1974; 35:896-901.
20. Goldstein SJ, DeJong JW. Changes in left ventricular wall dimensions during regional myocardial ischemia. *Am J Cardiol* 1974; 34:56-63.
21. Kerber RE, Marcus ML, Wilson R, et al. Effects of acute coronary occlusion on the motion and perfusion of the normal and ischemic interventricular septum. *Circulation* 1976; 54:928-935.
22. Mason SJ, Weiss JL, Weisfeldt ML, et al. Exercise echocardiography: detection of wall motion abnormalities during ischemia. *Circulation* 1979; 59:50-59.
23. Dicola VC, Downing SE, Donabedian RK, et al. Pathophysiological correlates of thallium-201 myocardial uptake in experimental infarction. *Cardiovasc Res* 1977; 11:141-146.
24. Beller GA, Cochavi S, Smith TW, et al. Positron emission tomography of the myocardium with  $^{81}\text{Rb}$ . *J Comput Assist Tomogr* 1982; 6:341-349.
25. Nishiyama H, Sodd VJ, Adolph RJ, et al. Intercomparison of myocardial imaging agents:  $^{201}\text{Tl}$ ,  $^{129}\text{Cs}$ ,  $^{43}\text{K}$ , and  $^{81}\text{Rb}$ . *J Nucl Med* 1976; 17:880-889.
26. Burch GE, Threefoot SA, Ray CT. The rate of disappearance of  $\text{Rb}^{86}$  from the plasma, the biologic decay rates of  $\text{Rb}^{86}$ , and the applicability of  $\text{Rb}^{86}$  as a tracer of potassium in man with and without chronic congestive failure. *J Lab Clin Med* 1955; 45:371-394.
27. Kilpatrick R, Renschler HE, Munro DS, et al. A comparison of the distribution of  $^{42}\text{K}$  and  $^{86}\text{Rb}$  in rabbits and man. *J Physiol* 1956; 133:194-201.
28. Becker L, Ferreira R, Thomas M. Comparison of  $^{86}\text{Rb}$  and microsphere estimates of left ventricular blood flow distribution. *J Nucl Med* 1975; 15:969-973.
29. Levy MN, deOliviera JM. Regional distribution of myocardial blood flow in the dog as determined by  $\text{Rb}^{86}$ . *Circ Res* 1961; 9:96-98.
30. Chu A, Murdock RH, Cobb FR. Relation between regional distribution of thallium-201 and myocardial blood flow in normal acutely ischemic and infarcted myocardium. *Am J Cardiol* 1982; 50:1141-1144.
31. Love WD, Burch GE. Influence of coronary plasma flow on the extraction of  $\text{Rb}^{81}$  from the coronary blood. *Circ Res* 1959; 7:24-30.
32. Jennings RB, Crout JR, Smetters GW. Studies on distribution and localization of potassium in early

- myocardial ischemic injury. *Arch Pathol* 1957; 63:586-592.
33. Goldhaber SZ, Newell JB, Ingwall JS, et al. Effects of reduced coronary flow on thallium-201 accumulation and release in an in vitro rat heart preparation. *Am J Cardiol* 1983; 51:891-902.
  34. Goldhaber SZ, Newell JB, Alpert NM, et al. Effect of ischemic-like insult on myocardial thallium-201 accumulation. *Circulation* 1983; 67:778-787.
  35. Jennings RB, Sommers HM, Kaltenbach JP, et al. Electrolyte alterations in acute myocardial ischemic injury. *Circ Res* 1964; 14:260-269.
  36. Britten JS, Blank M. Thallium activation of the (Na<sup>+</sup>-K<sup>+</sup>)-activated ATPase of rabbit kidney. *Biochem Biophys Acta* 1968; 159:160-166.
  37. Wisenberg GS, Schelbert HR, Hoffman EJ, et al. In vivo quantitation of regional myocardial blood flow by positron-emission computed tomography. *Circulation* 1981; 63:1248-1258.